IMA Journal of Numerical Analysis (2018) **00**, 1–25
doi:10.1093/imanum/dry041

A priori error for unilateral contact problems with Lagrange multipliers and isogeometric analysis

Pablo Antolin
EPFL SB MATHICSE MNS (Bât. MA), Station 8, CH 1015 Lausanne, Switzerland

Annalisa Buffa
Istituto di Matematica Applicata e Tecnologie Informatiche 'E. Magenes' del CNR via Ferrata 1, 27100, Pavia, Italy

and

Mathieu Fabre*
EPFL SB MATHICSE MNS (Bât. MA), Station 8, CH 1015 Lausanne, Switzerland
*Corresponding author: mathieu.fabre@epfl.ch.

[Received on 28 March 2017; revised on 4 May 2018]

In this paper we consider a unilateral contact problem without friction between a rigid body and a deformable one in the framework of isogeometric analysis. We present the theoretical analysis of the mixed problem. For the displacement, we use the pushforward of a nonuniform rational B-spline space of degree p and for the Lagrange multiplier, the pushforward of a B-spline space of degree $p-2$. These choices of space ensure the proof of an inf–sup condition and so on, the stability of the method. We distinguish between contact and noncontact sets to avoid the classical geometrical hypothesis of the contact set. An optimal *a priori* error estimate is demonstrated without assumption on the unknown contact set. Several numerical examples in two and three dimensions and in small and large deformation frameworks demonstrate the accuracy of the proposed method.

Keywords: unilateral contact problem; optimal *a priori* error; inf–sup condition; IGA; mixed IGA method; active set strategy; contact states.

1. Introduction

In the past few years the study of contact problems in small and large deformation frameworks has increased. The numerical solution of contact problems presents several difficulties: the computational cost, the high nonlinearity and the ill conditioning. Contrary to many other problems in nonlinear mechanics these problems cannot always be solved with a satisfactory level of robustness and accuracy (Laursen, 2003; Wriggers, 2006) using the numerical methods introduced.

One of the reasons that robustness and accuracy are hard to achieve is that the computation of gap, i.e. the distance between the deformed body and the obstacle, is indeed an ill-posed problem and its numerical approximation often introduces extra discontinuity which breaks the convergence of iterative schemes; see Alart & Curnier (1988); Laursen (2003); Wriggers (2006); Konyukhov & Schweizerhof (2013); Poulios & Renard (2015) where a master–slave method is introduced to weaken this effect.

In this respect the use of nonuniform rational B-spline (NURBS) or spline approximations within the framework of isogeometric analysis (Hughes *et al.*, 2005) holds great promise thanks to the increased regularity in the geometric description, which makes the gap computation intrinsically easier. Isogeometric analysis (IGA)-based methods use a generalisation of Bézier curves, B-spline and NURBS. These functions, used to represent the geometry of the domains with computer aided design (CAD), are used as basis functions to approximate partial differential equations; it is called the isoparametric paradigm. The smooth IGA basis functions possess a number of significant advantages for the analysis, including exact geometry and superior approximation. Isogeometric methods for frictionless contact problems have been introduced in Zavarise & Lorenzis (2009); Temizer *et al.* (2011, 2012); De Lorenzis *et al.* (2012); De Lorenzis *et al.* (2014); De Lorenzis *et al.* (2015); see also with primal and dual elements Wohlmuth (2000); Hüeber & Wohlmuth (2005); Hüeber *et al.* (2008); Popp *et al.* (2012); Seitz *et al.* (2016). Both point-to-segment and segment-to-segment (i.e. mortar type) algorithms have been designed and tested from an engineering perspective, showing that, indeed, the use of a smooth geometric representation helps the design of reliable methods for contact problems.

In this paper we take a slightly different point of view. Inspired by the recent design and analysis of isogeometric mortar methods in Brivadis *et al.* (2015) we consider a formulation of frictionless contact based on the choice of the Lagrange multiplier space proposed there. Indeed, we associate to NURBS displacement of degree p, a space of Lagrange multipliers of degree $p-2$. The use of lower-order multipliers has several advantages because it makes the evaluation of averaged gap values at active and inactive control points simpler, accurate and substantially more local. This choice of multipliers is then coupled with an active-set strategy, such as the one proposed and used in Hüeber & Wohlmuth (2005); Hüeber *et al.* (2008).

Moreover, it was assumed classically, that for the exact solution u there exist a finite number of points where the transition between contact and noncontact occurs. In the article Drouet & Hild (2015), contact and noncontact sets for the displacement are defined for the Signorini problem. This technique allows us to avoid an additional assumption for the unknown contact set in order to prove an *a priori* error estimate.

Finally, we perform a comprehensive set of tests both in small- and large-scale deformation frameworks, which show the performance of our method well. These tests have been performed with an in-house code developed upon the public library igatools (Pauletti *et al.*, 2015).

The outline of the paper is as follows: in Section 2, we introduce unilateral contact problem, some notation. In Section 3 we describe the discrete spaces and their properties. In Section 4 we present the theoretical analysis of the mixed problem. An optimal *a priori* error estimate without assumption on the unknown contact set is presented. In the last section, some two- and three-dimensional problems in a small deformation framework are presented in order to illustrate the convergence of the method with active-set strategy. A two-dimensional problem in a large deformation framework with neo-Hookean material law is provided to show the robustness of this method.

REMARK 1.1 The letter C stands for a generic constant, independent of the discretisation parameters and the solution u of the variational problem. For two scalar quantities a and b, the notation $a \lesssim b$ means there exists a constant C, independent of the mesh-size parameters, such that $a \leq Cb$. Moreover, $a \sim b$ means that $a \lesssim b$ and $b \lesssim a$.

2. Preliminaries and notation

2.1 *Unilateral contact problem*

Let $\Omega \subset \mathbb{R}^d$ (d =2 or 3) be a bounded regular domain which represents the reference configuration of a body submitted to a Dirichlet condition on Γ_D (with meas$(\Gamma_D) > 0$), a Neumann condition on Γ_N and a unilateral contact condition on a potential zone of contact Γ_C with a rigid body. Without loss of generality it is assumed that the body is subjected to a volume force f, to a surface traction ℓ on Γ_N and is clamped at Γ_D. Finally, we denote by n_Ω the unit outward normal vector on $\partial\Omega$.

In what follows we call u the displacement of Ω, $\varepsilon(u) = \frac{1}{2}(\nabla u + \nabla u^{\mathrm{T}})$ its linearised strain tensor and we denote by $\sigma = (\sigma_{ij})_{1\le i,j\le d}$ the stress tensor. We assume a linear constitutive law between σ and ε, i.e. $\sigma(u) = A\varepsilon(u)$, where $A = (a_{ijkl})_{1\le i,j,k,l\le d}$ is a fourth-order symmetric tensor verifying the usual bounds:

- $a_{ijkl} \in L^\infty(\Omega)$, i.e. there exists a constant m such that $\max\limits_{1\le i,j,k,l\le d} |a_{ijkl}| \le m$;
- there exists a constant $M > 0$ such that a.e. on Ω,

$$a_{ijkl}\varepsilon_{ij}\varepsilon_{kl} \ge M\varepsilon_{ij}\varepsilon_{ij} \quad \forall\,\varepsilon \in \mathbb{R}^{d\times d} \text{ with } \varepsilon_{ij} = \varepsilon_{ji}.$$

Let n be the outward unit normal vector at the rigid body. From now on we assume that n is an infinitely regular field. For any displacement field u and for any density of surface forces $\sigma(u)n$ defined on $\partial\Omega$ we adopt the following notation:

$$u = u_n n + u_t \qquad \text{and} \qquad \sigma(u)n = \sigma_n(u)n + \sigma_t(u),$$

where u_t (resp. $\sigma_t(u)$) are the tangential components with respect to n.

The unilateral contact problem between a rigid body and the elastic body Ω consists in finding the displacement u satisfying

$$\begin{aligned} \operatorname{div}\sigma(u) + f &= 0 && \text{in } \Omega,\\ \sigma(u) &= A\varepsilon(u) && \text{in } \Omega,\\ u &= 0 && \text{on } \Gamma_D,\\ \sigma(u)n_\Omega &= \ell && \text{on } \Gamma_N, \end{aligned} \tag{2.1}$$

and the conditions describing unilateral contact without friction at Γ_C are

$$\begin{aligned} u_n &\ge 0 && \text{(i)},\\ \sigma_n(u) &\le 0 && \text{(ii)},\\ \sigma_n(u)u_n &= 0 && \text{(iii)},\\ \sigma_t(u) &= 0 && \text{(iv)}. \end{aligned} \tag{2.2}$$

In order to describe the variational formulation of (2.1)–(2.2) we consider the Hilbert spaces

$$V := H^1_{0,\Gamma_D}(\Omega)^d = \left\{v \in H^1(\Omega)^d, \quad v = 0 \text{ on } \Gamma_D\right\}, \quad W = \left\{\, v_n|_{\Gamma_C}, \quad v \in V\right\},$$

and their dual spaces V', W' endowed with their usual norms. We denote

$$\|v\|_V = \left(\|v\|^2_{L^2(\Omega)^d} + |v|^2_{H^1(\Omega)^d}\right)^{1/2} \ \forall\, v \in V.$$

If $\overline{\Gamma}_D \cap \overline{\Gamma}_C = \emptyset$ and n is regular enough, it is well known that $W = H^{1/2}(\Gamma_C)$ and we denote W' by $H^{-1/2}(\Gamma_C)$. On the other hand, if $\overline{\Gamma}_D \cap \overline{\Gamma}_C \neq \emptyset$, it will hold that $H^{1/2}_{00}(\Gamma_C) \subset W \subset H^{1/2}(\Gamma_C)$. In all cases we will denote by $\|\cdot\|_W$ the norm on W and by $\langle\cdot,\cdot\rangle_{W',W}$ the duality pairing between W' and W. For all u and v in V we set

$$a(u,v) = \int_\Omega \sigma(u) : \varepsilon(v)\,\mathrm{d}\Omega \quad \text{and} \quad L(v) = \int_\Omega f\cdot v\,\mathrm{d}\Omega + \int_{\Gamma_N} \ell\cdot v\,\mathrm{d}\Gamma.$$

Let K_C be the closed convex cone of admissible displacement fields satisfying the noninterpenetration conditions, $K_C := \{v \in V, \quad v_n \geq 0 \text{ on } \Gamma_C\}$. A weak formulation of problem (2.1)–(2.2) (see Lions & Magenes, 1972), as a variational inequality, is to find $u \in K_C$ such that

$$a(u, v-u) \geq L(v-u) \qquad \forall\, v \in K_C. \tag{2.3}$$

We cannot directly use Newton–Raphson's method to solve formulation (2.3). A classical solution is to introduce a new variable, a Lagrange multipliers denoted by λ, which represent the surface normal force. For all λ in W' we denote $b(\lambda, v) = -\langle\lambda, v_n\rangle_{W',W}$ and M is the classical convex cone of multipliers on Γ_C:

$$M := \left\{\mu \in W', \quad \langle\mu,\psi\rangle_{W',W} \leq 0 \quad \forall\,\psi \in H^{1/2}(\Gamma_C), \quad \psi \geq 0 \text{ a.e. on } \Gamma_C\right\}.$$

The complementary conditions with Lagrange multipliers is written

$$\begin{aligned} u_n &\geq 0 \quad \text{(i)},\\ \lambda &\leq 0 \quad \text{(ii)},\\ \lambda u_n &= 0 \quad \text{(iii)}. \end{aligned} \tag{2.4}$$

The mixed formulation (Ben Belgacem & Renard, 2003) of the Signorini problem (2.1) and (2.4) consists in finding $(u,\lambda) \in V \times M$ such that

$$\begin{cases} a(u,v) - b(\lambda, v) = L(v), & \forall\, v \in V,\\ b(\mu-\lambda, u) \geq 0, & \forall\,\mu \in M. \end{cases} \tag{2.5}$$

Stampacchia's theorem ensures that problem (2.5) admits a unique solution.

The existence and uniqueness of the solution (u,λ) of the mixed formulation has been established in Haslinger *et al.* (1996) and it holds $\lambda = \sigma_n(u)$.

To simplify the notation we denote by $\|\cdot\|_{3/2+s,\Omega}$ the norm on $H^{3/2+s}(\Omega)^d$ and by $\|\cdot\|_{s,\Gamma_C}$ the norm on $H^s(\Gamma_C)$.

So, the following classical inequality (see Bazilevs *et al.*, 2006) holds.

THEOREM 2.1 Given $s > 0$ if the displacement u verifies $u \in H^{3/2+s}(\Omega)^d$, then $\lambda \in H^s(\Gamma_C)$ and it holds that

$$\|\lambda\|_{s,\Gamma_C} \leq \|u\|_{3/2+s,\Omega}\,. \tag{2.6}$$

The aim of this paper is to discretise problem (2.5) within the isogeometric paradigm, i.e. with splines and NURBS. Moreover, in order to properly choose the space of Lagrange multipliers we will be inspired by Brivadis *et al.* (2015). In what follows we introduce NURBS spaces and assumptions together with relevant choices of space pairings. In particular, following Brivadis *et al.* (2015), we concentrate on the definitions of B-spline displacements of degree p and multiplier spaces of degree $p-2$.

2.2 *NURBS discretisation*

In this section we describe briefly an overview of isogeometric analysis providing the notation and concepts needed in the next sections. Firstly, we define B-spline and NURBS in one dimension. Secondly, we extend these definitions to the multi dimensional case. Finally, we define the primal and the dual spaces for the contact boundary.

Let us denote by p the degree of univariate B-spline and by Ξ an open univariate knot vector, where the first and last entries are repeated $(p+1)$ times, i.e.

$$\Xi := \{0 = \xi_1 = \cdots = \xi_{p+1} < \xi_{p+2} \leq \cdots \leq \xi_\eta < \xi_{\eta+1} = \cdots = \xi_{\eta+p+1}\}.$$

Let us define $Z = \{\zeta_1, \ldots, \zeta_E\}$ as a vector of breakpoints, i.e. knots taken without repetition, and m_j as the multiplicity of the breakpoint ξ_j, $j = 1, \ldots, E$. Let Ξ be the open knot vector associated to Z where each breakpoint is repeated m_j times, i.e. in what follows we suppose that $m_1 = m_E = p+1$, while $m_j \leq p-1$ for all $j = 2, \ldots, E-1$. We define by $\hat{B}_i^p(\zeta)$, $i = 1, \ldots, \eta$ the ith univariable B-spline based on the univariate knot vector Ξ and the degree p. We denote $S^p(\Xi) = \mathrm{Span}\{\hat{B}_i^p(\zeta),\ i = 1, \ldots, \eta\}$. Moreover, for further use we denote by $\tilde{\Xi}$ the sub vector of Ξ obtained by removing the first and the last knots.

Multivariate B-spline in dimension d are obtained from the tensor product of univariate B-spline. For any direction $\delta \in \{1, \ldots, d\}$ we define by η_δ the number of B-spline, by Ξ_δ the open knot vector and by Z_δ the breakpoint vector. Then we define the multivariate knot vector by $\boldsymbol{\Xi} = (\Xi_1 \times \cdots \times \Xi_d)$ and the multivariate breakpoint vector by $\boldsymbol{Z} = (Z_1 \times \cdots \times Z_d)$. We introduce a set of multi-indices $\boldsymbol{I} = \{\boldsymbol{i} = (i_1, \ldots, i_d) \mid 1 \leq i_\delta \leq \eta_\delta\}$. We build the multivariate B-spline functions for each multi-index $\boldsymbol{i}$ by tensorisation from the univariate B-spline. Let $\boldsymbol{\zeta} \in \boldsymbol{Z}$ be a parametric coordinate of the generic point

$$\hat{B}_{\boldsymbol{i}}^p(\boldsymbol{\zeta}) = \hat{B}_{i_1}^p(\zeta_1) \ldots \hat{B}_{i_d}^p(\zeta_d).$$

Let us define the multivariate spline space in the reference domain by (for more details, see Brivadis *et al.*, 2015)

$$S^p(\boldsymbol{\Xi}) = \mathrm{Span}\{\hat{B}_{\boldsymbol{i}}^p(\boldsymbol{\zeta}),\ \boldsymbol{i} \in \boldsymbol{I}\}.$$

We define $N^p(\boldsymbol{\Xi})$ as the NURBS space spanned by the function $\hat{N}_{\boldsymbol{i}}^p(\boldsymbol{\zeta})$ with

$$\hat{N}_{\boldsymbol{i}}^p(\boldsymbol{\zeta}) = \frac{\omega_{\boldsymbol{i}} \hat{B}_{\boldsymbol{i}}^p(\boldsymbol{\zeta})}{\hat{W}(\boldsymbol{\zeta})},$$

where $\{\omega_{\boldsymbol{i}}\}_{\boldsymbol{i} \in \boldsymbol{I}}$ is a set of positive weights and $\hat{W}(\boldsymbol{\zeta}) = \sum_{\boldsymbol{i} \in \boldsymbol{I}} \omega_{\boldsymbol{i}} \hat{B}_{\boldsymbol{i}}^p(\boldsymbol{\zeta})$ is the weight function and we set

$$N^p(\boldsymbol{\Xi}) = \mathrm{Span}\{\hat{N}_{\boldsymbol{i}}^p(\boldsymbol{\zeta}),\ \boldsymbol{i} \in \boldsymbol{I}\}.$$

In what follows we will assume that Ω is obtained as the image of $\hat{\Omega} =]0,1[^d$ through a NURBS mapping φ_0, i.e. $\Omega = \varphi_0(\hat{\Omega})$. Moreover, in order to simplify our presentation, we assume that Γ_C is the image of a full face $\hat{f}$ of $\bar{\hat{\Omega}}$, i.e. $\Gamma_C = \varphi_0(\hat{f})$. We denote by φ_{0,Γ_C} the restriction of φ_0 to $\hat{f}$.

A NURBS surface, in $d = 2$, or solid, in $d = 3$, is parameterised by

$$\mathcal{C}(\boldsymbol{\zeta}) = \sum_{\boldsymbol{i}\in\boldsymbol{I}} C_{\boldsymbol{i}} \hat{N}^p_{\boldsymbol{i}}(\boldsymbol{\zeta}),$$

where $C_{\boldsymbol{i}\in\boldsymbol{I}} \in \mathbb{R}^d$ is a set of control point coordinates. The control points are somewhat analogous to nodal points in finite element analysis. The NURBS geometry is defined as the image of the reference domain $\hat{\Omega}$ by φ, called a geometric mapping, $\Omega_t = \varphi(\hat{\Omega})$.

We remark that the physical domain Ω is split into elements by the image of $\mathbf{Z}$ through the map φ_0. We denote such a physical mesh by $\mathcal{Q}_h$ and physical elements in this mesh will be called Q; Γ_C inherits a mesh that we denote by $\mathcal{Q}_h|_{\Gamma_C}$. Elements on this mesh will be denoted Q_C.

Finally, we introduce some notation and assumptions on the mesh.

ASSUMPTION 2.2 The mapping φ_0 is considered to be a bi-Lipschitz homeomorphism. Furthermore, for any parametric element $\hat{Q}$, $\varphi_0|_{\bar{\hat{Q}}}$ is in $\mathcal{C}^\infty(\bar{\hat{Q}})$ and for any physical element Q, $\varphi_0^{-1}|_{\bar{Q}}$ is in $\mathcal{C}^\infty(\bar{Q})$.

Let h_Q be the size of a physical element Q; it holds that $h_Q = \mathrm{diam}(Q)$. In the same way we define the mesh size for any parametric element. In addition, Assumption 2.2 ensures that both sizes of mesh are equivalent. We denote the maximal mesh size by $h = \max_{Q\in\mathcal{Q}_h} h_Q$.

ASSUMPTION 2.3 The mesh $\mathcal{Q}_h$ is quasi-uniform, i.e. there exists a constant θ such that $\frac{h_Q}{h_{Q'}} \leq \theta$ with Q and $Q' \in \mathcal{Q}_h$.

3. Discrete spaces and their properties

We concentrate now on the definition of spaces on the domain Ω.

For displacements we denote by $V^h \subset V$ the space of mapped NURBS of degree p with appropriate homogeneous Dirichlet boundary condition:

$$V^h := \left\{ v^h = \hat{v}^h \circ \varphi_0^{-1}, \quad \hat{v}^h \in N^p(\boldsymbol{\Xi})^d \right\} \cap V.$$

We denote the space of traces normal to the rigid body by

$$W^h := \left\{ \psi^h, \quad \exists\, v^h \in V^h : \quad v^h \cdot n = \psi^h \text{ on } \Gamma_C \right\}.$$

For multipliers, following the ideas of Brivadis *et al.* (2015), we define the space of B-spline of degree $p-2$ on the potential contact zone $\Gamma_C = \varphi_{0,\Gamma_C}(\hat{f})$. We denote by $\boldsymbol{\Xi}_{\hat{f}}$ the knot vector defined on $\hat{f}$ and by $\tilde{\boldsymbol{\Xi}}_{\hat{f}}$ the knot vector obtained by removing the first and last value in each knot vector. We define

$$\Lambda^h := \left\{ \lambda^h = \hat{\lambda}^h \circ \varphi_{0,\Gamma_C}^{-1}, \quad \hat{\lambda}^h \in S^{p-2}(\tilde{\boldsymbol{\Xi}}_{\hat{f}}) \right\}.$$

The scalar space Λ^h is spanned by mapped B-spline of the type $\hat{B}^{p-2}_{\boldsymbol{i}}(\boldsymbol{\zeta}) \circ \varphi_{0,\Gamma_C}^{-1}$ for $\boldsymbol{i}$ belonging to a suitable set of indices. In order to reduce our notation we call K the unrolling of the multi-index $\boldsymbol{i}$,

$K = 0, \ldots, \mathcal{K}$ and remove super-indices; for K corresponding to a given $\boldsymbol{i}$, we set $\hat{B}_K(\boldsymbol{\zeta}) = \hat{B}_{\boldsymbol{i}}^{p-2}(\boldsymbol{\zeta})$, $B_K = \hat{B}_K \circ \varphi_{0,\Gamma_C}^{-1}$ and

$$\Lambda^h := \mathrm{Span}\{B_K(x), \quad K = 0, \ldots, \mathcal{K}\}. \tag{3.1}$$

For further use, for $v \in L^2(\Gamma_C)$ and for each $K = 0, \ldots, \mathcal{K}$, we denote by $\left(\Pi_\lambda^h \cdot\right)_K$ the weighted average of v,

$$\left(\Pi_\lambda^h v\right)_K = \frac{\int_{\Gamma_C} v B_K \,\mathrm{d}\Gamma}{\int_{\Gamma_C} B_K \,\mathrm{d}\Gamma}, \tag{3.2}$$

and by Π_λ^h a global operator such as

$$\Pi_\lambda^h v = \sum_{K=0}^{\mathcal{K}} \left(\Pi_\lambda^h v\right)_K B_K. \tag{3.3}$$

We denote by L^h the subset of W^h on which the non-negativity holds only at the control points:

$$L^h = \left\{\varphi^h \in W^h, \quad \left(\Pi_\lambda^h \varphi^h\right)_K \geq 0 \quad \forall K\right\}.$$

We note that L^h is a convex subset of W^h.

Next we define the discrete space of Lagrange multipliers as the negative cones of L^h by

$$M^h := L^{h,*} = \left\{\mu^h \in \Lambda^h, \quad \int_{\Gamma_C} \mu^h \varphi^h \,\mathrm{d}\Gamma \leq 0 \quad \forall \varphi^h \in L^h\right\}.$$

For any $Q_C \in \mathcal{Q}_h|_{\Gamma_C}$, $\tilde{Q}_C$ denotes the support extension of Q_C (see Bazilevs *et al.*, 2006; Beirão da Veiga *et al.*, 2014) defined as the image of supports of B-spline that are not zero on $\hat{Q}_C = \varphi_{0,\Gamma_C}^{-1}(Q_C)$. We notice that the operator verifies the following estimate error.

Lemma 3.1 Let $\psi \in H^s(\Gamma_C)$ with $0 \leq s \leq 1$; the estimate for the local interpolation error reads

$$\left\|\psi - \Pi_\lambda^h(\psi)\right\|_{0,Q_C} \lesssim h^s \left\|\psi\right\|_{s,\tilde{Q}_C} \qquad \forall Q_C \in \mathcal{Q}_h|_{\Gamma_C}. \tag{3.4}$$

Proof. First, let c be a constant. It holds that

$$\Pi_\lambda^h c \;=\; \sum_{K=0}^{\mathcal{K}} \left(\Pi_\lambda^h c\right)_K B_K = \sum_{K=0}^{\mathcal{K}} \frac{\int_{\Gamma_C} c B_K \,\mathrm{d}\Gamma}{\int_{\Gamma_C} B_K \,\mathrm{d}\Gamma} B_K = \sum_{K=0}^{\mathcal{K}} c \frac{\int_{\Gamma_C} B_K \,\mathrm{d}\Gamma}{\int_{\Gamma_C} B_K \,\mathrm{d}\Gamma} B_K = c \sum_{K=0}^{\mathcal{K}} B_K.$$

Using that B-spline are a partition of unity we obtain $\Pi_\lambda^h c = c$.
Let $\psi \in H^s(\Gamma_C)$; it holds that

$$\begin{aligned}\left\|\psi - \Pi_\lambda^h(\psi)\right\|_{0,Q_C} &= \left\|\psi - c - \Pi_\lambda^h(\psi - c)\right\|_{0,Q_C} \\ &\le \|\psi - c\|_{0,Q_C} + \left\|\Pi_\lambda^h(\psi - c)\right\|_{0,Q_C}\end{aligned}. \tag{3.5}$$

We need now to bound the operator Π_λ^h. We obtain

$$\begin{aligned}\left\|\Pi_\lambda^h(\psi - c)\right\|_{0,Q_C} &= \left\|\sum_{K=0}^{\mathcal{K}} \frac{\int_{\Gamma_C}(\psi - c)B_K \,\mathrm{d}\Gamma}{\int_{\Gamma_C} B_K \,\mathrm{d}\Gamma} B_K\right\|_{0,Q_C} \\ &\le \sum_{K:\ \mathrm{supp}B_K \cap Q_C \neq \emptyset}^{\mathcal{K}} \left|\frac{\int_{\Gamma_C}(\psi - c)B_K \,\mathrm{d}\Gamma}{\int_{\Gamma_C} B_K \,\mathrm{d}\Gamma}\right| \|B_K\|_{0,Q_C} \\ &\le \sum_{K:\ \mathrm{supp}B_K \cap Q_C \neq \emptyset}^{\mathcal{K}} \|(\psi - c)\|_{0,\tilde{Q}_C} \frac{\|B_K\|_{0,\tilde{Q}_C}}{\int_{\Gamma_C} B_K \,\mathrm{d}\Gamma} \|B_K\|_{0,Q_C}\,.\end{aligned}$$

Using $\|B_K\|_{0,\tilde{Q}_C} \sim \left|\tilde{Q}_C\right|^{1/2}$, $\|B_K\|_{0,Q_C} \sim |Q_C|^{1/2}$, $\int_{\Gamma_C} B_K \,\mathrm{d}\Gamma \sim \left|\tilde{Q}_C\right|$ and Assumption 2.2 it holds that

$$\left\|\Pi_\lambda^h(\psi - c)\right\|_{0,Q_C} \lesssim \|(\psi - c)\|_{0,\tilde{Q}_C}\,. \tag{3.6}$$

Using the previous inequalities (3.5) and (3.6), for $0 \le s \le 1$, we obtain

$$\left\|\psi - \Pi_\lambda^h(\psi)\right\|_{0,Q_C} \lesssim \|\psi - c\|_{0,\tilde{Q}_C} \lesssim h_{\tilde{Q}_C}^s |\psi|_{s,\tilde{Q}_C}\,.$$

□

PROPOSITION 3.2 For h sufficiently small there exists a $\beta > 0$ such that

$$\inf_{\mu^h \in M^h} \sup_{\psi^h \in W^h} \frac{-\int_{\Gamma_C} \psi^h \mu^h \,\mathrm{d}\Gamma}{\left\|\psi^h\right\|_{0,\Gamma_C} \left\|\mu^h\right\|_{0,\Gamma_C}} \ge \beta. \tag{3.7}$$

Proof. In the article Brivadis *et al.* (2015) the authors prove that, if h is sufficiently small, there exists a constant β independent of h such that

$$\forall \phi^h \in (\Lambda^h)^d, \quad \exists u^h \in V^h\big|_{\Gamma_C} \quad \text{s.t.} \quad \frac{-\int_{\Gamma_C} \phi^h \cdot u^h \,\mathrm{d}\Gamma}{\left\|u^h\right\|_{0,\Gamma_C}} \ge \beta \left\|\phi^h\right\|_{0,\Gamma_C}. \tag{3.8}$$

Given now a $\lambda^h \in \Lambda^h$ and $\psi^h \in W^h$ we should like to choose $\phi^h = \lambda^h n$ and $\psi^h = u^h \cdot n$ in (3.8), but, unfortunately, it is clear that $\phi^h \notin (\Lambda^h)^d$. Indeed, (3.7) can obtained from (3.8) via a superconvergence argument that we discuss in the next lines.

Let $\Pi_{(\Lambda^h)^d} : L^2(\Gamma_C)^d \to (\Lambda^h)^d$ be a quasi-interpolant defined and studied in, e.g., Beirão da Veiga *et al.* (2014).
If $n \in W^{p-1,\infty}(\Gamma_C)$, by the same superconvergence argument used in Brivadis *et al.* (2015), we obtain

$$\left\|\phi^h - \Pi_{(\Lambda^h)^d}(\phi^h)\right\|_{0,\Gamma_C} \le \alpha h \left\|\phi^h\right\|_{0,\Gamma_C}. \tag{3.9}$$

Note that

$$\begin{aligned} b(\lambda^h, u^h) &= -\int_{\Gamma_C} \lambda^h(u^h \cdot n)\, \mathrm{d}\Gamma = -\int_{\Gamma_C} \phi^h \cdot u^h\, \mathrm{d}\Gamma \\ &= -\int_{\Gamma_C} \Pi_{(\Lambda^h)^d}(\phi^h) \cdot u^h\, \mathrm{d}\Gamma - \int_{\Gamma_C} \left(\phi^h - \Pi_{(\Lambda^h)^d}(\phi^h)\right) \cdot u^h\, \mathrm{d}\Gamma. \end{aligned}$$

By the inf–sup condition (3.8) we get

$$\sup_{u^h \in V^h} \frac{-\int_{\Gamma_C} \Pi_{(\Lambda^h)^d}(\phi^h) \cdot u^h\, \mathrm{d}\Gamma}{\left\|u^h\right\|_{0,\Gamma_C}} \ge \beta \left\|\Pi_{(\Lambda^h)^d}(\phi^h)\right\|_{0,\Gamma_C}.$$

By (3.9), it holds that

$$\int_{\Gamma_C} \left(\phi^h - \Pi_{(\Lambda^h)^d}(\phi^h)\right) \cdot u^h\, \mathrm{d}\Gamma \le \alpha h \|\phi^h\|_{0,\Gamma_C} \|u^h\|_{0,\Gamma_C}.$$

Thus,

$$\frac{b(\lambda^h, u^h)}{\|u^h\|_{0,\Gamma_C}} \ge \beta \left\|\Pi_{(\Lambda^h)^d}(\phi^h)\right\|_{0,\Gamma_C} - \alpha h \left\|\phi^h\right\|_{0,\Gamma_C}.$$

Noting that $\left\|\Pi_{(\Lambda^h)^d}(\phi^h)\right\|_{0,\Gamma_C} \ge \left\|\phi^h\right\|_{0,\Gamma_C} - \alpha h \left\|\phi^h\right\|_{0,\Gamma_C}$ (see Brivadis *et al.* (2015), for more details) and using that $\left\|\phi^h\right\|_{0,\Gamma_C} \sim \left\|\lambda^h\right\|_{0,\Gamma_C}$ and $\left\|u^h\right\|_{0,\Gamma_C} \sim \left\|\psi^h\right\|_{0,\Gamma_C}$, we obtain finally

$$\sup_{u^h \in V^h} \frac{-\int_{\Gamma_C} \psi^h \lambda^h\, \mathrm{d}\Gamma}{\|\psi^h\|_{0,\Gamma_C}} \ge \beta \left\|\lambda^h\right\|_{0,\Gamma_C} - \alpha h \left\|\lambda^h\right\|_{0,\Gamma_C}.$$

For h sufficiently small this implies that there exists a constant β' independent of h such that

$$\sup_{u^h \in V^h} \frac{-\int_{\Gamma_C} \psi^h \lambda^h\, \mathrm{d}\Gamma}{\|\psi^h\|_{0,\Gamma_C}} \ge \beta' \left\|\lambda^h\right\|_{0,\Gamma_C}. \tag{3.10}$$

□

Lemma 3.3 For h sufficiently small, M^h can be characterised as

$$M^h \equiv \left\{\mu^h \in \Lambda^h, \quad \mu^h = \sum_K \mu_K^h B_K, \quad \mu_K^h \le 0\right\}.$$

Proof. Let $\mu^h \in M^h$. For all $\varphi^h \in W^h$, we have

$$\int_{\Gamma_C} \mu^h \varphi^h \, \mathrm{d}\Gamma = \sum_K \int_{\Gamma_C} \mu_K^h B_K \varphi^h \, \mathrm{d}\Gamma = \sum_K \mu_K^h \left(\Pi_\lambda^h \varphi^h\right)_K \int_{\Gamma_C} B_K \, \mathrm{d}\Gamma.$$

Let us recall that $\left(\Pi_\lambda^h \varphi^h\right)_K = \int_{\Gamma_C} \varphi^h B_K \, \mathrm{d}\Gamma / \int_{\Gamma_C} B_K \, \mathrm{d}\Gamma$ where B_K are the basis functions of the multipliers on Γ_C.

For each K, K' we wish to construct a φ_K^h such that

$$\left(\Pi_\lambda^h \varphi_K^h\right)_{K'} = \delta_{K,K'}. \tag{3.11}$$

Clearly, such a φ_K^h, if it exists, belongs to L^h by construction. Moreover, as $\mu^h \in M^h$, $\int_{\Gamma_C} \mu^h \varphi_K^h \, \mathrm{d}\Gamma = \mu_K^h \int_{\Gamma_C} B_K \, \mathrm{d}\Gamma \leq 0$, i.e. $\mu_K^h \leq 0$.

Now, it remains to construct φ_K^h verifying (3.11).
By definition of $\left(\Pi_\lambda^h \cdot\right)_K$, such a φ_K^h has to verify

$$\int_{\Gamma_C} \varphi_K^h B_{K'} \, \mathrm{d}\Gamma = \delta_{K,K'} \int_{\Gamma_C} B_{K'} \, \mathrm{d}\Gamma, \tag{3.12}$$

and the existence of such φ_K^h is guaranteed by the inf–sup condition. Indeed, it guarantees that the rectangular system (3.12) is solvable as the matrix is full rank. □

Then a discretised mixed formulation of problem (2.5) consists in finding $(u^h, \lambda^h) \in V^h \times M^h$ such that

$$\begin{cases} a(u^h, v^h) - b(\lambda^h, v^h) = L(v^h) & \forall\, v^h \in V^h, \\ b(\mu^h - \lambda^h, u^h) \geq 0 & \forall\, \mu^h \in M^h. \end{cases} \tag{3.13}$$

According to Lemma 3.3, we get

$$\{\mu^h \in M^h : \quad b(\mu^h, v^h) = 0 \quad \forall\, v^h \in V^h)\} = \{0\},$$

and using the ellipticity of the bilinear form $a(\cdot,\cdot)$ on V^h, then problem (3.13) admits a unique solution $(u^h, \lambda^h) \in V^h \times M^h$.

Before addressing the analysis of (3.13) let us recall that the following inequalities (see Bazilevs *et al.*, 2006) are true for the primal and the dual space.

THEOREM 3.4 Given a quasi-uniform mesh and let r, s be such that $0 \leq r \leq s \leq p+1$. Then there exists a constant depending only on p, θ, φ_0 and $\hat{W}$ such that for any $v \in H^s(\Omega)$ there exists an approximation $v^h \in V^h$ such that

$$\left\| v - v^h \right\|_{r,\Omega} \lesssim h^{s-r} \left\| v \right\|_{s,\Omega}. \tag{3.14}$$

We will also make use of local approximation estimates for spline quasi-interpolants which can be found, e.g., in Bazilevs *et al.* (2006); Beirão da Veiga *et al.* (2014).

LEMMA 3.5 Let $\lambda \in H^s(\Gamma_C)$ with $0 \leq s \leq p-1$; then there exists a constant depending only on p, φ_0 and θ, and there exists an approximation $\lambda^h \in \Lambda^h$ such that

$$h^{-1/2}\left\|\lambda - \lambda^h\right\|_{-1/2,Q_C} + \left\|\lambda - \lambda^h\right\|_{0,Q_C} \lesssim h^s \left\|\lambda\right\|_{s,\tilde{Q}_C} \qquad \forall\, Q_C \in \mathcal{Q}_h|\Gamma_C. \tag{3.15}$$

It is well known (Boffi *et al.*, 2013) that the stability for the mixed problem (2.5) is linked to the inf–sup condition.

THEOREM 3.6 For h sufficiently small, n sufficiently regular and for any $\mu^h \in \Lambda^h$, it holds that

$$\sup_{v^h \in V^h} \frac{b(\mu^h, v^h)}{\left\|v^h\right\|_V} \geq \beta \left\|\mu^h\right\|_{W'}, \tag{3.16}$$

where β is independent of h.

Proof. By Proposition 3.2 there exists a Fortin operator $\Pi : L^2(\Gamma_C) \to V^h|_{\Gamma_C} \cap H^1_0(\Gamma_C)$ such that

$$b(\lambda, \Pi(u)) = b(\lambda, u)\ \forall\, \lambda \in M \quad \text{and} \quad \|\Pi(u)\|_{0,\Gamma_C} \leq \|u\|_{0,\Gamma_C}.$$

Let I_h be an L^2 and H^1 stable quasi-interpolant onto $V^h|_{\Gamma_C}$ (e.g., the Schumaker quasi-interpolant; see for more details Beirão da Veiga *et al.*, 2014). It is important to notice that I^h preserves the homogeneous Dirichlet boundary condition.
We set $\Pi_F = \Pi(I - I_h) + I_h$. It is classical to see that

$$b(\lambda, \Pi_F(u)) = b(\lambda, u) \quad \forall\, \lambda \in M, \tag{3.17}$$

and it is easy to see that

$$\Pi_F(u^h) = u^h \quad \forall\, u^h \in V^h|_{\Gamma_C}. \tag{3.18}$$

Moreover, by stability of Π and I_h, it holds that

$$\|\Pi_F(u)\|_{0,\Gamma_C} \lesssim \|u\|_{0,\Gamma_C} \quad \forall\, u \in L^2(\Gamma_C), \tag{3.19}$$

and also

$$\|\Pi_F(u)\|_{1,\Gamma_C} \lesssim \|(u)\|_{1,\Gamma_C} \quad \forall\, u \in H^1(\Gamma_C). \tag{3.20}$$

To conclude we distinguish between two cases:

- If $\overline{\Gamma}_D \cap \overline{\Gamma}_C = \emptyset$ it is well known that $W = H^{1/2}(\Gamma_C)$. By interpolation of Sobolev spaces, using (3.19) and (3.20), we obtain

$$b(\lambda, \Pi_F(u)) = b(\lambda, u) \quad \forall\, \lambda \in M \quad \text{and} \quad \|\Pi_F(u)\|_W \lesssim \|u\|_W.$$

  Then the inf–sup condition (3.16) holds thanks to Boffi *et al.* (2013, Proposition 5.4.2).

- If $\overline{\Gamma}_D \cap \overline{\Gamma}_C \neq \emptyset$, it is enough to recall that for all $u \in H^1_{0,\Gamma_D\cap\Gamma_C}(\Gamma_C)$, we have $\Pi_F(u) \in H^1_{0,\Gamma_D\cap\Gamma_C}(\Gamma_C)$ and (3.20) is valid on the subspace $H^1_{0,\Gamma_D\cap\Gamma_C}(\Gamma_C)$. Again by an interpolation argument between (3.19) and (3.20) it holds that $\|\Pi_F(u)\|_W \leq C\,\|u\|_W$, which ends the proof. □

4. *A priori* error analysis

In this section we present an optimal *a priori* error estimate for the Signorini mixed problem. Our estimates follows the ones for finite elements provided in Coorevits *et al.* (2002); Hild & Laborde (2002), and refined in Drouet & Hild (2015). In particular, in Drouet & Hild (2015), the authors overcome a technical assumption on the geometric structure of the contact set and we are able to avoid such assumptions in our case also.

Indeed, for any p, we prove our method to be optimal for solutions with regularity up to $5/2$. Thus, optimality for the displacement is obtained for any $p \geq 2$. The cheapest and more convenient method proved optimal corresponds to the choice $p = 2$. Larger values of p may be of interest because they produce continuous pressures, but, on the other hand, the error bounds remain limited by the regularity of the solution, i.e. up to $Ch^{3/2}$. Clearly, to enhance approximation, suitable local refinement may be used (De Lorenzis *et al.*, 2012), but this choice is outside the scope of this paper.

In order to prove Theorem 4.3 which follows we need a few preparatory lemmas. First, we introduce some notation and some basic estimates. Let us define the active-set strategy for the variational problem. Given an element $Q_C \in \mathcal{Q}_h|_{\Gamma_C}$ of the undeformed mesh we denote by $Z_C(Q_C)$ the contact set and by $Z_{\mathrm{NC}}(Q_C)$ the noncontact set in Q_C as follows:

$$Z_C(Q_C) = \{x \in Q_C, \quad u_n(x) = 0\} \quad \text{and} \quad Z_{\mathrm{NC}}(Q_C) = \{x \in Q_C, \quad u_n(x) > 0\}.$$

Here, $|Z_C(Q_C)|$ and $|Z_{\mathrm{NC}}(Q_C)|$ stand for their measures and $|Z_C(Q_C)| + |Z_{\mathrm{NC}}(Q_C)| = |Q_C| = Ch_{Q_C}^{d-1}$.

Remark 4.1 Since u_n belongs to $H^{1+\nu}(\Omega)^2$ for $0 < \nu < 1$, if $d = 2$ the Sobolev embeddings ensure that $u_n \in \mathcal{C}^0(\partial\Omega)$. It implies that $Z_C(Q_C)$ and $Z_{\mathrm{NC}}(Q_C)$ are measurable as inverse images of a set by a continuous function.

The following estimates are the generalisation to the mixed problem of Drouet & Hild (2015, Lemma 2 of the appendix). We recall that if (u, λ) is a solution of the mixed problem (2.5), then $\sigma_n(u) = \lambda$. So, the following lemma can be proved in exactly the same way.

Lemma 4.2 Let $d = 2$ or 3. Let (u, λ) be the solution of the mixed formulation (2.5) and let $u \in H^{3/2+\nu}(\Omega)^d$ with $0 < \nu < 1$. Let h_Q be the diameter of the trace element Q_C and the set of contact $Z_C(Q_C)$ and noncontact $Z_{\mathrm{NC}}(Q_C)$ defined previously in Q_C.
We assume that $|Z_{\mathrm{NC}}(Q_C)| > 0$; the following L^2-estimate holds for λ:

$$\|\lambda\|_{0,Q_C} \leq \frac{1}{|Z_{\mathrm{NC}}(Q_C)|^{1/2}} h_{Q_C}^{d/2+\nu-1/2} |\lambda|_{\nu,Q_C}. \tag{4.1}$$

We assume that $|Z_C(Q_C)| > 0$; the following L^2-estimates hold for ∇u_n:

$$\|\nabla u_n\|_{0,Q_C} \leq \frac{1}{|Z_C(Q_C)|^{1/2}} h_{Q_C}^{d/2+\nu-1/2} |\nabla u_n|_{\nu,Q_C}. \tag{4.2}$$

THEOREM 4.3 Let (u, λ) and (u^h, λ^h) be the solution of the mixed problem (2.5) and the discrete mixed problem (3.13), respectively. Assume that $u \in H^{3/2+\nu}(\Omega)^d$ with $0 < \nu < 1$. Then the following error estimate is satisfied:

$$\left\|u - u^h\right\|_V^2 + \left\|\lambda - \lambda^h\right\|_{W'}^2 \lesssim h^{1+2\nu} \left\|u\right\|_{3/2+\nu,\Omega}^2 . \tag{4.3}$$

Proof. In Hild & Laborde (2002, Proposition 4.1) it is proved that if (u, λ) is the solution of the mixed problem (2.5) and (u^h, λ^h) is the solution of the discrete mixed problem (3.13), it holds that

$$\begin{aligned}\left\|u - u^h\right\|_V^2 + \left\|\lambda - \lambda^h\right\|_{W'}^2 \lesssim\ & \left\|u - v^h\right\|_V^2 + \left\|\lambda - \mu^h\right\|_{W'}^2 \\ & + \max(-b(\lambda, u^h), 0) + \max(-b(\lambda^h, u), 0).\end{aligned}$$

It remains to estimate the last two terms in the previous inequality to obtain the estimate (4.3).

Step 1: Estimate of $-b(\lambda, u^h) = \int_{\Gamma_C} \lambda u_n^h \, \mathrm{d}\Gamma$.

Using the operator Π_λ^h defined in (3.3) it holds that

$$\begin{aligned} -b(\lambda, u^h) &= \int_{\Gamma_C} \lambda u_n^h \, \mathrm{d}\Gamma = \int_{\Gamma_C} \lambda \left(u_n^h - \Pi_\lambda^h(u_n^h)\right) \mathrm{d}\Gamma + \int_{\Gamma_C} \lambda \Pi_\lambda^h(u_n^h) \, \mathrm{d}\Gamma \\ &= \int_{\Gamma_C} \left(\lambda - \Pi_\lambda^h(\lambda)\right)\left(u_n^h - \Pi_\lambda^h(u_n^h)\right) \mathrm{d}\Gamma + \int_{\Gamma_C} \Pi_\lambda^h(\lambda)\left(u_n^h - \Pi_\lambda^h(u_n^h)\right) \mathrm{d}\Gamma \\ &\quad + \int_{\Gamma_C} \lambda \Pi_\lambda^h(u_n^h) \, \mathrm{d}\Gamma. \end{aligned}$$

Since λ is a solution of (2.5) it holds that $\Pi_\lambda^h(\lambda) \leq 0$. Furthermore, u^h is a solution of (3.13), thus $\int_{\Gamma_C} \Pi_\lambda^h(\lambda)\left(u_n^h - \Pi_\lambda^h(u_n^h)\right) \mathrm{d}\Gamma \leq 0$ and $\int_{\Gamma_C} \lambda \Pi_\lambda^h(u_n^h) \, \mathrm{d}\Gamma \leq 0$.
We obtain

$$\begin{aligned} -b(\lambda, u^h) &\leq \int_{\Gamma_C} \left(\lambda - \Pi_\lambda^h(\lambda)\right)\left(u_n^h - \Pi_\lambda^h(u_n^h)\right) \mathrm{d}\Gamma \\ &\leq \int_{\Gamma_C} \left(\lambda - \Pi_\lambda^h(\lambda)\right)\left(u_n^h - u_n - \Pi_\lambda^h(u_n^h - u_n)\right) \mathrm{d}\Gamma \\ &\quad + \int_{\Gamma_C} \left(\lambda - \Pi_\lambda^h(\lambda)\right)\left(u_n - \Pi_\lambda^h(u_n)\right) \mathrm{d}\Gamma. \end{aligned} \tag{4.4}$$

The first term of (4.4) is bounded in an optimal way by using (3.4), the summation on each physical element, Theorem 2.1 and the trace theorem:

$$\begin{aligned} \int_{\Gamma_C} \left(\lambda - \Pi_\lambda^h(\lambda)\right)\left(u_n^h - u_n - \Pi_\lambda^h(u_n^h - u_n)\right) \mathrm{d}\Gamma &\leq \left\|\lambda - \Pi_\lambda^h(\lambda)\right\|_{0,\Gamma_C} \left\|u_n^h - u_n - \Pi_\lambda^h(u_n^h - u_n)\right\|_{0,\Gamma_C} \\ &\leq C h^{1/2+\nu} \left\|\lambda\right\|_{\nu,\Gamma_C} \left\|u_n - u_n^h\right\|_W \\ &\leq C h^{1/2+\nu} \left\|u\right\|_{3/2+\nu,\Omega} \left\|u - u^h\right\|_V . \end{aligned}$$

We need now to bound the second term in (4.4). Let Q_C be an element of $\mathcal{Q}_h|_{\Gamma_C}$. If either $|Z_C(Q_C)|$ or $|Z_{\mathrm{NC}}(Q_C)|$ are null the integral on Q_C vanishes. So we suppose that either $|Z_C(Q_C)|$ or $|Z_{\mathrm{NC}}(Q_C)|$ are greater than $|Q_C|/2 = Ch_{Q_C}^{d-1}$ and we consider the two cases, separately.

Similarly to the article Hild & Laborde (2002) we can prove that if

- $|Z_C(Q_C)| \geq |Q_C|/2$, using estimate (3.4), estimate (4.2) of Lemma 4.2 and Young's inequality, it holds that

$$\int_{Q_C} \left(\lambda - \Pi_\lambda^h(\lambda)\right)\left(u_n - \Pi_\lambda^h(u_n)\right) \, \mathrm{d}\Gamma \lesssim h^{1+2\nu} \left(\|\lambda\|^2_{\nu,Q_C} + \|u_n\|^2_{1+\nu,\tilde{Q}_C} \right).$$

- $|Z_{\mathrm{NC}}(Q_C)| \geq |Q_C|/2$, using estimate (3.4), estimate (4.1) of Lemma 4.2 and Young's inequality, it holds that

$$\int_{Q_C} \left(\lambda - \Pi_\lambda^h(\lambda)\right)\left(u_n - \Pi_\lambda^h(u_n)\right) \, \mathrm{d}\Gamma \lesssim h^{1+2\nu} \left(\|\lambda\|^2_{\nu,\tilde{Q}_C} + \|u_n\|^2_{1+\nu,\tilde{Q}_C} \right).$$

Summing over all the contact elements and distinguishing between the two cases $Z_C(Q_C) \geq |Q_C|/2$ and $Z_{\mathrm{NC}}(Q_C) \geq |Q_C|/2$, it holds that

$$\begin{aligned}
\int_{\Gamma_C} \left(\lambda - \Pi_\lambda^h(\lambda)\right)\left(u_n - \Pi_\lambda^h(u_n)\right) \, \mathrm{d}\Gamma &= \sum_{Q_C \in \mathcal{Q}_h|_{\Gamma_C}} \int_{Q_C} \left(\lambda - \Pi_\lambda^h(\lambda)\right)\left(u_n - \Pi_\lambda^h(u_n)\right) \, \mathrm{d}\Gamma \\
&\leq Ch^{1+2\nu} \sum_{Q_C \in \mathcal{Q}_h|_{\Gamma_C}} \|\lambda\|^2_{\nu,Q_C} + \|\lambda\|^2_{\nu,\tilde{Q}_C} + \|u_n\|^2_{1+\nu,\tilde{Q}_C} \\
&\leq Ch^{1+2\nu} \sum_{Q_C \in \mathcal{Q}_h|_{\Gamma_C}} \|\lambda\|^2_{\nu,Q_C} + \sum_{Q'_C \in \tilde{Q}_C} \|\lambda\|^2_{\nu,Q'_C} + \|u_n\|^2_{1+\nu,Q'_C} \\
&\leq Ch^{1+2\nu} \left(\|\lambda\|^2_{\nu,\Gamma_C} + \sum_{Q \in \mathcal{Q}_h|_{\Gamma_C}} \sum_{Q'_C \in \tilde{Q}_C} \|\lambda\|^2_{\nu,Q'_C} + \|u_n\|^2_{1+\nu,Q'_C} \right).
\end{aligned}$$

Due to the compact supports of the B-spline basis functions there exists a constant C depending only on the degree p and the dimension d of the undeformed domain such that

$$\sum_{Q \in \mathcal{Q}_h|_{\Gamma_C}} \sum_{Q'_C \in \tilde{Q}_C} \|\lambda\|^2_{\nu,Q'_C} + \|u_n\|^2_{1+\nu,Q'_C} \leq C \|\lambda\|^2_{\nu,\Gamma_C} + C \|u_n\|^2_{1+\nu,\Gamma_C}.$$

So we have

$$\int_{\Gamma_C} \left(\lambda - \Pi_\lambda^h(\lambda)\right)\left(u_n - \Pi_\lambda^h(u_n)\right) \, \mathrm{d}\Gamma \leq Ch^{1+2\nu} \left(\|\lambda\|^2_{\nu,\Gamma_C} + \|u_n\|^2_{1+\nu,\Gamma_C} \right),$$

i.e.

$$\int_{\Gamma_C} \big(\lambda - \Pi_\lambda^h(\lambda)\big)\big(u_n - \Pi_\lambda^h(u_n)\big)\,\mathrm{d}\Gamma \le Ch^{1+2\nu}\,\|u\|^2_{3/2+\nu,\Omega}\,.$$

We conclude that

$$-b(\lambda, u^h) \lesssim h^{1/2+\nu}\,\|u\|_{3/2+\nu,\Omega}\,\big\|u-u^h\big\|_V + h^{1+2\nu}\,\|u\|^2_{3/2+\nu,\Omega}\,.$$

Using Young's inequality we obtain

$$-b(\lambda, u^h) \lesssim h^{1+2\nu}\,\|u\|^2_{3/2+\nu,\Omega} + \big\|u-u^h\big\|^2_V\,. \tag{4.5}$$

Step 2: Estimate of $-b(\lambda^h, u) = \int_{\Gamma_C} \lambda^h u_n\,\mathrm{d}\Gamma$.
Let us denote by j^h the Lagrange interpolation operator of order 1 on $\mathcal{Q}_h|_{\Gamma_C}$,

$$-b(\lambda^h, u) = \int_{\Gamma_C} \lambda^h u_n\,\mathrm{d}\Gamma = \int_{\Gamma_C} \lambda^h\big(u_n - j^h(u_n)\big)\,\mathrm{d}\Gamma + \int_{\Gamma_C} \lambda^h j^h(u_n)\,\mathrm{d}\Gamma.$$

Note that by Remark 4.1, u_n is continuous and $j^h(u_n)$ is well defined.
Since u is a solution of (2.5) it holds that $j^h(u_n) \ge 0$. Thus, $\int_{\Gamma_C} \lambda^h j^h(u_n)\,\mathrm{d}\Gamma \le 0,\ \lambda^h \in M^h$.
As previously we obtain

$$\begin{aligned}
-b(\lambda^h, u) &\le \int_{\Gamma_C} \lambda^h u_n\,\mathrm{d}\Gamma \le \int_{\Gamma_C} \lambda^h\big(u_n - j^h(u_n)\big)\,\mathrm{d}\Gamma \\
&\le \int_{\Gamma_C} (\lambda^h - \lambda)\big(u_n - j^h(u_n)\big)\,\mathrm{d}\Gamma + \int_{\Gamma_C} \lambda\big(u_n - j^h(u_n)\big)\,\mathrm{d}\Gamma \\
&\le \int_{\Gamma_C} \lambda\big(u_n - j^h(u_n)\big)\,\mathrm{d}\Gamma + \big\|\lambda-\lambda^h\big\|_{W'}\,\big\|u_n - j^h(u_n)\big\|_W \\
&\le \int_{\Gamma_C} \lambda\big(u_n - j^h(u_n)\big)\,\mathrm{d}\Gamma + h^{1/2+\nu}\,\|u_n\|_{1+\nu,\Gamma_C}\,\big\|\lambda-\lambda^h\big\|_{W'} \\
&\le \int_{\Gamma_C} \lambda\big(u_n - j^h(u_n)\big)\,\mathrm{d}\Gamma + h^{1/2+\nu}\,\|u\|_{3/2+\nu,\Omega}\,\big\|\lambda-\lambda^h\big\|_{W'}\,.
\end{aligned}$$

Now we need to show

$$\int_{\Gamma_C} \lambda\big(u_n - j^h(u_n)\big)\,\mathrm{d}\Gamma \le Ch^{1+2\nu}\,\|u\|^2_{3/2+\nu,\Omega}\,. \tag{4.6}$$

The proof of this inequality is given in Drouet & Hild (2015) for both linear and quadratic finite elements, and can be repeated here verbatim. In this proof two cases are considered:

1. either $|Z_C(Q_C)|$ or $|Z_{\mathrm{NC}}(Q_C)|$ is null and thus the inequality is trivial;
2. either $|Z_C(Q_C)|$ or $|Z_{\mathrm{NC}}(Q_C)|$ is greater than $|Q_C|/2 = Ch^{d-1}_{Q_C}$.

As previously, choosing either $|Z_C(Q_C)|$ or $|Z_{NC}(Q_C)|$, using Lemma 4.2 and by summation on all elements of the mesh we conclude that

$$\begin{aligned} -b(\lambda^h, u) &\leq \int_{\Gamma_C} \lambda(u_n - j^h(u_n))\, \mathrm{d}\Gamma + h^{1/2+\nu} \|u\|_{3/2+\nu,\Omega} \left\|\lambda - \lambda^h\right\|_{W'} \\ &\lesssim h^{1+2\nu} \|u\|^2_{3/2+\nu,\Omega} + h^{1/2+\nu} \|u\|_{3/2+\nu,\Omega} \left\|\lambda - \lambda^h\right\|_{W'}. \end{aligned}$$

Using Young's inequality we obtain

$$-b(\lambda^h, u) \lesssim h^{1+2\nu} \|u\|^2_{3/2+\nu,\Omega} + \left\|\lambda - \lambda^h\right\|^2_{W'}. \tag{4.7}$$

Finally, we can conclude using (4.7) and (4.5). □

5. Numerical study

In this section we perform a numerical validation for the method we proposed in small as well as in large deformation frameworks, i.e. also beyond the theory developed in previous sections. Due to the intrinsic lack of regularity of contact solutions we restrict ourselves to the case $p = 2$, for which the N_2/S_0 method is tested.

The suite of benchmarks reproduces the classical Hertz contact problem (Hertz, 1882): Sections 5.1 and 5.1 analyse the two- and three-dimensional cases for a small deformation setting, whereas Section 5.3 considers the large deformation problem in two dimensions. The examples were performed using an in-house code based on the igatools library (see Pauletti *et al.*, 2015 for further details).

In the following example, to prevent the contact zone being empty, we considered, only for the initial gap, that there exists contact if $g_n \leq 10^{-9}$.

5.1 *Two-dimensional Hertz problem*

The example included in this section analyses the two-dimensional frictionless Hertz contact problem considering small elastic deformations. It consists of an infinitely long half cylinder body with radius $R = 1$, which is deformable and whose material is linear elastic, with Young's modulus $E = 1$ and Poisson's ratio $\nu = 0.3$. A uniform pressure $P = 0.003$ is applied on the top face of the cylinder while the curved surface contacts a horizontal rigid plane (see Fig. 1(a)). Taking into account the test symmetry and the ideally infinite length of the cylinder, the problem is modelled as a two-dimensional quarter of a disc with proper boundary conditions.

Under the hypothesis that the contact area is small compared to the cylinder dimensions, Hertz's analytical solution (see Hertz, 1882) predicts that the contact region is an infinitely long band of width $2a$, with $a = \sqrt{8R^2P(1-\nu^2)/\pi E}$. Thus, the normal pressure, which follows an elliptical distribution along the width direction r, is $p(r) = p_0\sqrt{1 - r^2/a^2}$, where the maximum pressure, at the central line of the band ($r = 0$), is $p_0 = 4RP/\pi a$. For the geometrical, material and load data chosen in this numerical test the characteristic values of the solution are $a = 0.083378$ and $p_0 = 0.045812$. Notice that, as required by Hertz's theory hypotheses, a is sufficiently small compared to R.

It is important to remark that, despite the fact that Hertz's theory provides a full description of the contact area and the normal contact pressure in the region, it does not describe analytically the deformation of the whole elastic domain. Therefore, for all the test cases hereinafter, the L^2error norm

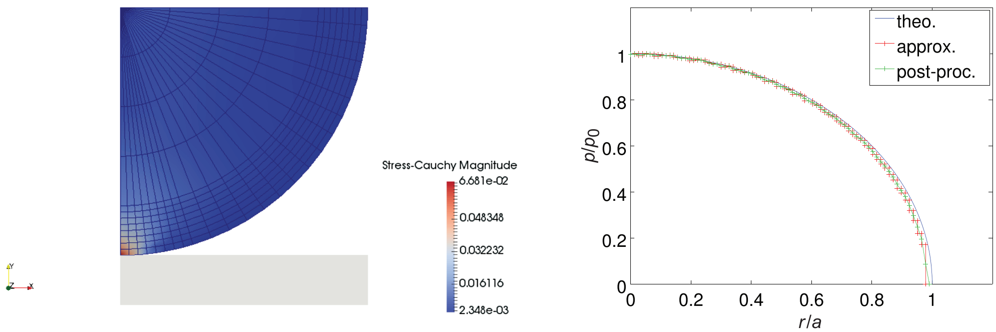

(a) Stress magnitude distribution for the undeformed mesh. (b) Analytical and numerical contact pressure.

FIG. 1. Two-dimensional Hertz contact problem with N_2/S_0 method for an applied pressure $P = 0.003$.

and H^1error seminorm of the displacement obtained numerically are computed taking a more refined solution as a reference. For this bidimensional test case the mesh size of the refined solution h_{ref} is such that, for all the discretizations, $4h_{\text{ref}} \leq h$, where h is the size of the mesh considered. Additionally, as shown in Fig. 1(a), the mesh is finer in the vicinity of the potential contact zone. The knot vector values are defined such that 80% of the knot spans are located within 10% of the total length of the knot vector.

In particular, the analysis of this example focuses on the effect of the interpolation order on the quality of contact stress distribution. Thus, in Fig. 1(b) we compare the pressure reference solution. with the Lagrange multiplier values computed at the control points, i.e. its constant values, and a post processing that consists of a $P1$ re interpolation. The dimensionless contact pressure p/p_0 is plotted with respect to the normalised coordinate r/a. The results are very good; the maximum pressure computed and the pressure distribution, even across the boundary of the contact region (in the contact and noncontact zones), are close to the analytical solution.

In Fig. 2(a) absolute errors in L^2-norm and H^1-seminorm for the N_2/S_0 choice are shown. As expected, optimal convergence is obtained for the displacement error in the H^1-seminorm; the convergence rate is close to the expected $3/2$ value. Nevertheless, the L^2-norm of the displacement error presents suboptimal convergence (close to 2), but according to Aubin–Nitsche's lemma in the linear case the expected convergence rate is lower than $5/2$. On the other hand, in Fig. 2(b) the L^2-norm of the Lagrange multipliers error is presented; the expected convergence rate is 1, whereas a convergence rate close to 0.6 is achieved when we compare the numerical solution and Hertz's analytical solution, and close to 0.8 is achieved when we compare the numerical solution and the refined numerical solution.

5.2 *Three-dimensional Hertz problem*

In this section the three-dimensional frictionless Hertz problem is studied. It consists of a hemispherical elastic body with radius R that contacts a horizontal rigid plane as a consequence of a uniform pressure P applied on the top face (see Fig. 3(a)). Hertz's theory predicts that the contact region is a circle of radius $a = (3R^3P(1-\nu^2)/4E)^{1/3}$ and the contact pressure follows a hemispherical distribution $p(r) = p_0\sqrt{1 - r^2/a^2}$, with $p_0 = 3R^2P/2a^2$, with r the distance to the centre of the circle (see Hertz, 1882). In this case for the chosen values $R = 1$, $E = 1$, $\nu = 0.3$ and $P = 10^{-4}$, the contact radius is $a = 0.059853$ and the maximum pressure $p_0 = 0.041872$. As in the two-dimensional case, Hertz's theory relies on the hypothesis that a is small compared to R and the deformations are small.

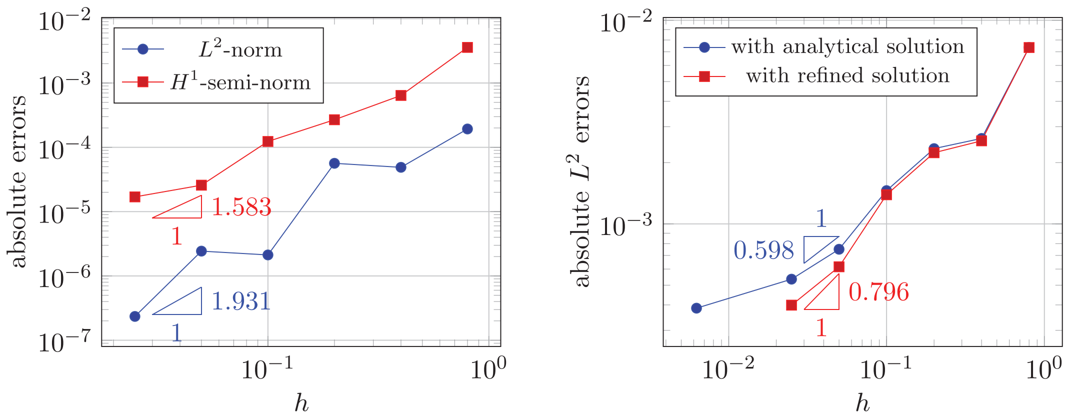

(a) Displacement error. (b) Lagrange multipliers error.

FIG. 2. Two-dimensional Hertz contact problem with N_2/S_0 method for an applied pressure $P = 0.003$. Absolute displacement errors in L^2-norm and H^1-seminorm and Lagrange multipliers error in L^2-norm, with respect to analytical and refined numerical solutions.

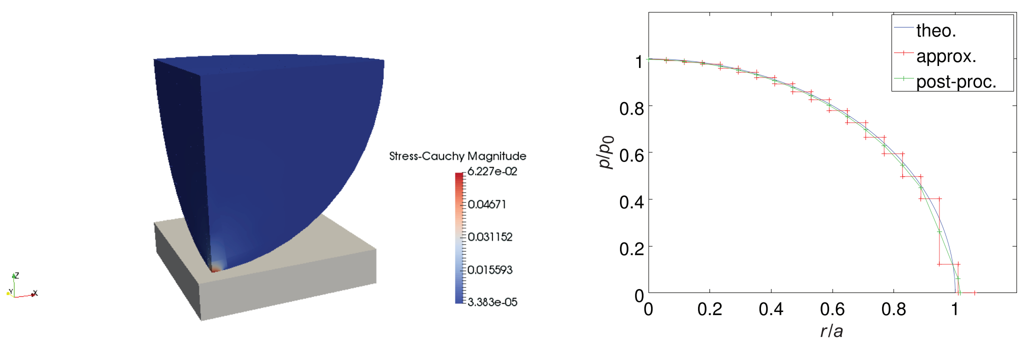

(a) magnitude for the undeformed mesh. (b) Analytical and numerical contact pressure for $h = 0.1$.

FIG. 3. Three-dimensional Hertz contact problem with N_2/S_0 method for an applied pressure $P = 10^{-4}$.

Considering the problem's axial symmetry, the test is reproduced using an octant of a sphere with proper boundary conditions. Figure 3(a) shows the problem set-up and the magnitude of the computed stresses. As in the two-dimensional case, in order to achieve more accurate results in the contact region, the mesh is refined in the vicinity of the potential contact zone. The knot vectors are defined such that 75% of the elements are located within 10% of the total length of the knot vector.

In Fig. 3(b) we compare Hertz's solution with the computed contact pressure at control points and a $P1$ re interpolation of those values, for a mesh with size $h = 0.1$. On the other hand, in Fig. 4 the contact pressure is shown at control points for mesh sizes $h = 0.4$ and $h = 0.2$. As can be appreciated, good agreement between the analytical and computed pressures is obtained in all cases.

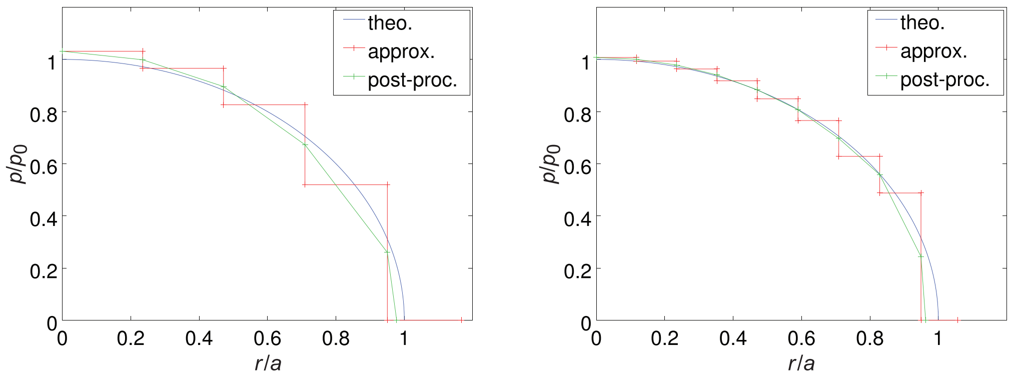

(a) $h = 0.4$.
(b) $h = 0.2$.

FIG. 4. Three-dimensional Hertz contact problem with N_2/S_0 method for an applied pressure $P = 10^{-4}$. Contact pressure solution at control points.

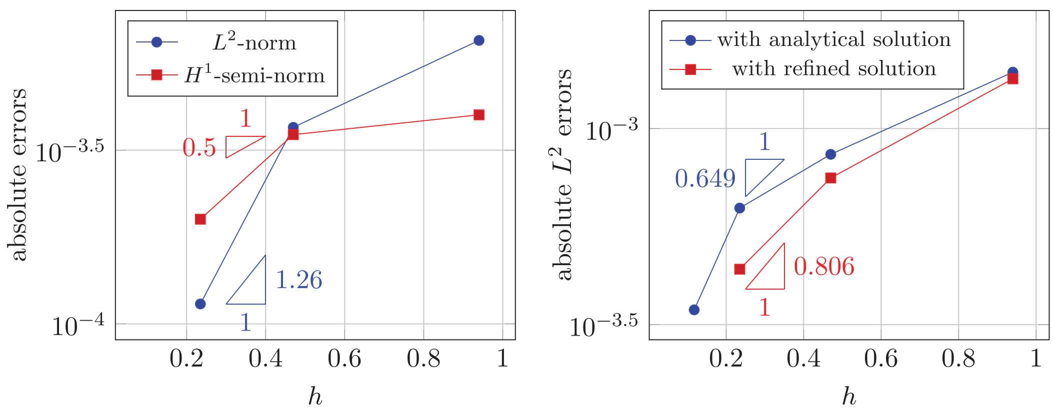

(a) Displacement error.
(b) Lagrange multipliers error.

FIG. 5. Three-dimensional Hertz contact problem with N_2/S_0 method for an applied pressure $P = 10^{-4}$. Absolute displacement errors in L^2-norm and H^1-seminorm and Lagrange multipliers error in L^2-norm, with respect to analytical and refined numerical solutions.

As in the previous test the displacement of the deformed elastic body is not fully described by Hertz's theory. Therefore, the L^2 error norm and H^1 error seminorm of the displacement are evaluated by comparing the obtained solution with a more refined case. Nonetheless, Lagrange multipliers computed solutions are compared with the analytical contact pressure. In this test case the size of the refined mesh is $h_{\text{ref}} = 0.1175$ (0.0025 in the contact region), and it is such that $2h_{\text{ref}} \leq h$.

In Fig. 5(a) the displacement error norms are reported. As can be seen they present suboptimal convergence rates both in the L^2-norm and H^1-seminorm. Convergence rates are close to 1.26 and 0.5, respectively. The large mesh size of the numerical reference solution h_{ref}, limited by our computational resources, seems to be the cause of these suboptimal results. Due to the coarse reference mesh the

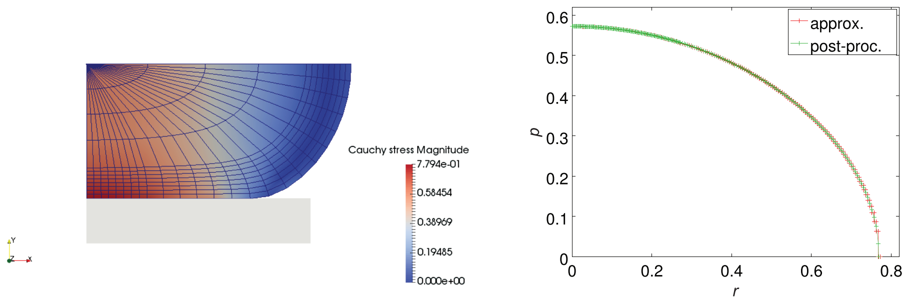

(a) Stress magnitude distribution for the deformed mesh.

(b) Analytical and numerical contact pressure for $h = 0.1$

FIG. 6. Two-dimensional large deformation Hertz contact problem with N_2/S_0 method with a uniform downward displacement $u_y = -0.4$.

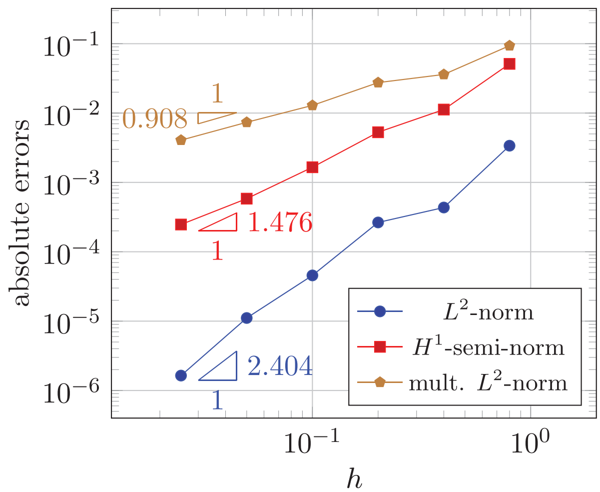

FIG. 7. Two-dimensional large deformation Hertz contact problem with N_2/S_0 method with a uniform downward displacement $u_y = -0.4$. Absolute displacement errors in L^2-norm and H^1-seminorm and Lagrange multipliers error in L^2-norm.

presented rates are only pre-asymptotic. Better behaviour is observed for the Lagrange multipliers error (Fig. 5(b)).

5.3 *Two-dimensional Hertz problem with large deformations*

Finally, in this section the two-dimensional frictionless Hertz problem is studied considering large deformations and strains. For that purpose a neo-Hookean material constitutive law (a hyper-elastic law that considers finite strains) with Young's modulus $E = 1$ and Poisson's ratio $\nu = 0.3$ has been used for the deformable body.

As in Section 5.1 the performance of the N_2/S_0 method is analysed and the problem is modelled as an elastic quarter of a disc with proper boundary conditions. The considerations made about the mesh size in Section 5.1 are also valid for the present case. The radius of the cylinder is $R = 1$ but modifying its boundary conditions; instead of pressure, a uniform downward displacement $u_y = -0.4$ is applied on the top surface of the cylinder. In this large deformation framework the exact solution is unknown; the errors of the computed displacement and Lagrange multipliers are studied taking a refined numerical solution as reference. The large deformation of the body and computed contact pressure are presented in Fig. 6.

In Fig. 7 the displacement and multiplier errors are reported. It can be seen that the obtained displacement presents optimal convergence both in L^2-norm and H^1-semi norm; analogously, optimal convergence is also achieved for the computed Lagrange multipliers.

Conclusions

In this work we present an optimal *a priori* error estimate of a unilateral frictionless contact problem between a deformable body and a rigid one.

For the numerical point of view we observed that this method is optimal for both variables, the displacement and the Lagrange multipliers. In our experiments, we used basis functions of degree 2 for the primal space and B-spline of degree 0 for the dual space. Thanks to this choice of approximation spaces we observed stability for the Lagrange multipliers and optimal approximation of the pressure in the two-dimensional case and suboptimal pre-asymptotic convergence in the three-dimensional one. The suboptimality observed in the three-dimensional case may be due to the coarse mesh used. This NURBS-based contact formulation seems to provide a robust description for the large deformations setting.

Funding

Michelin (A10-4087); European Research Council (694515 to A.B.); Progetti di Ricerca di Interesse Nazionale-Ministero dell'Istruzione dell'Università e della Ricerca project 'Metodologie innovative nella modellistica differenziale numerica'.

References

Alart, P. & Curnier, A. (1988) A generalized Newton method for contact problems with friction. *J. Mécanique Théor. Appl.*, **7**, 67–82.

Bazilevs, Y., Beirao da Veiga, L., Cottrell, J. A., Hughes, T. J. R. & Sangalli, G. (2006) Isogeometric analysis: approximation, stability and error estimates for h-refined meshes. *Math. Models Methods Appl. Sci.*, **16**, 1031–1090.

Beirao da Veiga, L., Buffa, A., Sangalli, G. & Vázquez, R. (2014) Mathematical analysis of variational isogeometric methods. *Acta Numer.*, **23**, 157–287.

Ben Belgacem, F. & Renard, Y. (2003) Hybrid finite element methods for the Signorini problem. *Math. Comp.*, **72**, 1117–1145.

Boffi, D., Brezzi, F. & Fortin, M. (2013) *Mixed Finite Element Methods and Applications.* Springer Series in Computational Mathematics, vol. 44. Berlin, Heidelberg: Springer.

Brivadis, E., Buffa, A., Wohlmuth, B. & Wunderlich, L. (2015) Isogeometric mortar methods. *Comput. Methods Appl. Mech. Engrg.*, **284**, 292–319.

Coorevits, P., Hild, P., Lhalouani, K. & Sassi, T. (2002) Mixed finite element methods for unilateral problems: convergence analysis and numerical studies. *Math. Comp.*, **71**, 67–82.

De Lorenzis, L., Evans, J., Hughes, T. & Reali, A. (2015) Isogeometric collocation: Neumann boundary conditions and contact. *Comput. Methods Appl. Mech. Engrg.*, **284**, 21–54.

De Lorenzis, L., Wriggers, P. & Hughes, T. J. (2014) Isogeometric contact: a review. *GAMM-Mitteilungen*, **37**, 85–123.

De Lorenzis, L., Wriggers, P. & Zavarise, G. (2012) A mortar formulation for 3D large deformation contact using NURBS-based isogeometric analysis and the augmented Lagrangian method. *Comput. Mech.*, **49**, 1–20.
Drouet, G. & Hild, P. (2015) Optimal convergence for discrete variational inequalities modelling Signorini contact in 2D and 3D without additional assumptions on the unknown contact set. *SIAM J. Numer. Anal.*, **53**, 1488–1507.
Haslinger, J., Hlaváček, I. & Nečas, J. (1996) Numerical methods for unilateral problems in solid mechanics. *Handbook of Numerical Analysis* (P. G. Ciarlet & J. L. Lions eds.), vol. 4, ch. 2. North-Holland: Elsevier, pp. 313–485.
Hertz, H. (1882) Über die Berührung fester elastischer Körper. *J. Reine Angew. Math.*, **92**, 156–171.
Hild, P. & Laborde, P. (2002) Quadratic finite element methods for unilateral contact problems. *Appl. Numer. Math.*, **41**, 401–421.
Hüeber, S., Stadler, G. & Wohlmuth, B. I. (2008) A primal-dual active set algorithm for three-dimensional contact problems with Coulomb friction. *SIAM J. Sci. Comput.*, **30**, 572–596.
Hüeber, S. & Wohlmuth, B. I. (2005) A primal–dual active set strategy for non-linear multibody contact problems. *Computer Methods in Applied Mechanics and Engineering.*, **194**, 3147–3166.
Hughes, T. J. R., Cottrell, J. A. & Bazilev, Y. (2005) Isogeometric analysis: CAD, finite elements, NURBS, exact geometry and mesh refinement. *Comput. Methods Appl. Mech. Engrg.*, **194**, 4135–4195.
Konyukhov, A. & Schweizerhof, K. (2013) *Computational contact mechanics*. Geometrically Exact Theory for Arbitrary Shaped Bodies. Lecture Notes in Applied and Computational Mechanics, vol. 67. Berlin, Heidelberg: Springer.
Laursen, T. A. (2003) *Computational Contact and Impact Mech*. Berlin: Springer.
Lions, J. L. & Magenes, E. (1972) *Non-homogeneous Boundary Value Problems and Applications*. Berlin, New York: Springer.
Pauletti, M. S., Martinelli, M., Cavallini, N. & Antolin, P. (2015) Igatools: an isogeometric analysis library. *SIAM J. Sci. Comput.*, **37**, C465–C496.
Popp, A., Wohlmuth, B. I., Gee, M. W. & Wall, W. A. (2012) Dual quadratic mortar finite element methods for 3D finite deformation contact. *SIAM J. Sci. Comput.*, **34**, B421–B446.
Poulios, K. & Renard, Y. (2015) An unconstrained integral approximation of large sliding frictional contact between deformable solids. *Comput. & Structures*, **153**, 75–90.
Seitz, A., Farah, P., Kremheller, J., Wohlmuth, B. I., Wall, W. A. & Popp, A. (2016) Isogeometric dual mortar methods for computational contact mechanics. *Comput. Methods Appl. Mech. Engrg.*, **301**, 259–280.
Temizer, I., Wriggers, P. & Hughes, T. (2011) Contact treatment in isogeometric analysis with NURBS. *Comput. Methods Appl. Mech. Engrg.*, **200**, 1100–1112.
Temizer, I., Wriggers, P. & Hughes, T. (2012) Three-dimensional mortar-based frictional contact treatment in isogeometric analysis with NURBS. *Comput. Methods Appl. Mech. Engrg.*, **209–212**, 115–128.
Wohlmuth, B. I. (2000) A mortar finite element method using dual spaces for the Lagrange multiplier. *SIAM J. Numer. Anal.*, **38**, 989–1012.
Wriggers, P. (2006) *Computational Contact Mechanics,* 2nd edn. Berlin, Heidelberg: Springer.
Zavarise, G. & Lorenzis, L. D. (2009) The node-to-segment algorithm for 2D frictionless contact: classical formulation and special cases. *Comput. Methods Appl. Mech. Engrg.*, **79**, 379–416.

Appendix

In this appendix we provide the ingredients needed to fully discretise problem (3.13) as well as its large deformation version that we used in Section 5. First we introduce the contact status, an active-set strategy for the discrete problem, and then the fully discrete problem. For the purpose of this appendix we take notation suitable to large deformations and denote by g_n the distance between the rigid and the deformable body. For small deformations it holds that $g_n(u) = u \cdot n$.

Contact status

Let us first deal with the contact status. The active-set strategy is defined in Hüeber *et al.* (2008); Hüeber & Wohlmuth (2005) and is updated at each Newton iteration. Due to the deformation, parts of the workpiece may come into contact or conversely may lose contact. This change of contact status changes the loading that is applied on the boundary of the mesh. This method is used to track the location of contact during the change in boundary conditions.
Let K be a control point of the B-spline space (3.1); let $\left(\Pi_\lambda^h \cdot\right)_K$ be the local projection defined in (3.2) and let $P\left\{\lambda_K, \left(\Pi_\lambda^h g_n\right)_K\right\}$ be the operator defined componentwise by

- $\lambda_K = 0$;
  (1) if $\left(\Pi_\lambda^h g_n\right)_K \geq 0$ then $P\left\{\lambda_K, \left(\Pi_\lambda^h g_n\right)_K\right\} = 0$;
  (2) if $\left(\Pi_\lambda^h g_n\right)_K < 0$ then $P\left\{\lambda_K, \left(\Pi_\lambda^h g_n\right)_K\right\} = \left(\Pi_\lambda^h g_n\right)_K$;
- $\lambda_K < 0$;
  (3) $P\left\{\lambda_K, \left(\Pi_\lambda^h g_n\right)_K\right\} = \left(\Pi_\lambda^h g_n\right)_K$.

The optimality conditions are then written $P\left\{\lambda_K, \left(\Pi_\lambda^h g_n\right)_K\right\} = 0$. So in case (1) the constraints are inactive and in cases (2) and (3) the constraints are active.

Discrete problem

The space V^h is spanned by mapped NURBS of type $\hat{N}_{\boldsymbol{i}}^p(\boldsymbol{\zeta}) \circ \varphi_{0,\Gamma_C}^{-1}$ for $\boldsymbol{i}$ belonging to a suitable set of indices. In order to simplify and reduce our notation we call A the running index, of control points associated with the surface $\Gamma_C, A = 0, \ldots, \mathcal{A}$ on this basis and set

$$V^h = \operatorname{Span}\{N_A(x), \quad A = 0, \ldots, \mathcal{A}\} \cap V. \tag{A.1}$$

Now we express quantities on the contact interface Γ_C as

$$u|_{\Gamma_C} = \sum_{A=1}^{\mathcal{A}} u_A N_A, \qquad \delta u|_{\Gamma_C} = \sum_{A=1}^{\mathcal{A}} \delta u_A N_A \qquad \text{and} \qquad x = \sum_{A=1}^{\mathcal{A}} x_A N_A,$$

where C_A, u_A, δu_A and $x_A = \varphi(X_A)$ are the related reference coordinate, displacement, displacement variation and current coordinate vectors.

By substituting the interpolations the normal gap becomes

$$g_n = \left[\sum_{A=1}^{\mathcal{A}} C_A N_A(\zeta) + \sum_{A=1}^{\mathcal{A}} u_A N_A(\zeta)\right] \cdot n.$$

In the previous equation, ζ are the parametric coordinates of the generic point on Γ_C. To simplify the notation, we denote for the next of the purpose $\mathcal{D}g_n[\delta u]$ by δg_n. The virtual variation follows as

$$\delta g_n = \left[\sum_{A=1}^{\mathcal{A}} \delta u_A N_A(\zeta)\right] \cdot n.$$

In order to formulate the problem in matrix form the following vectors are introduced:

$$\delta \boldsymbol{u} = \begin{bmatrix} \delta u_1 \\ \vdots \\ \delta u_{\mathcal{A}} \end{bmatrix}, \qquad \Delta \boldsymbol{u} = \begin{bmatrix} \Delta u_1 \\ \vdots \\ \Delta u_{\mathcal{A}} \end{bmatrix}, \qquad \boldsymbol{N} = \begin{bmatrix} N_1(\zeta) n \\ \vdots \\ N_{\mathcal{A}}(\zeta) n \end{bmatrix}.$$

With the above notation the virtual variation and the linearised increments can be written in matrix form as

$$\delta g_n = \delta \boldsymbol{u}^{\mathrm{T}} \boldsymbol{N}, \qquad \Delta g_n = \boldsymbol{N}^{\mathrm{T}} \Delta \boldsymbol{u}.$$

The contact contribution of the virtual work is expressed

$$\delta W_c = \int_{\Gamma_C} \lambda \delta g_n \, \mathrm{d}\Gamma + \int_{\Gamma_C} \delta \lambda g_n \, \mathrm{d}\Gamma.$$

The discretised contact contribution can be expressed

$$\begin{aligned}
\delta W_c &= \int_{\Gamma_C} \sum_{K=1}^{\mathcal{K}} \lambda_K B_K \delta g_n \, \mathrm{d}\Gamma + \int_{\Gamma_C} \sum_{K=1}^{\mathcal{K}} \delta \lambda_K B_K g_n \, \mathrm{d}\Gamma \\
&= \sum_K \lambda_K \int_{\Gamma_C} B_K \delta g_n \, \mathrm{d}\Gamma + \delta \lambda_K \int_{\Gamma_C} B_K g_n \, \mathrm{d}\Gamma \\
&= \sum_K \lambda_K \int_{\Gamma_C} B_K \delta g_n \, \mathrm{d}\Gamma + \delta \lambda_K \int_{\Gamma_C} B_K g_n \, \mathrm{d}\Gamma \\
&= \sum_K \Big(\lambda_K \big(\Pi_\lambda^h \delta g_n\big)_K + \delta \lambda_K \big(\Pi_\lambda^h g_n\big)_K \Big) K_K,
\end{aligned}$$

where $K_K = \int_{\Gamma_C} B_K \, \mathrm{d}\Gamma$.
Indeed, we need to resolve a variational inequality. Using the contact status we distinguish between constraints on the control point K which are actives, i.e. when contact occurs, and constraints on the control point K which are inactives, i.e. when we lose contact.

Using active-set strategy on the local gap $\big(\Pi_\lambda^h g_n\big)_K$ and λ_K, it holds that

$$\delta W_c = \sum_{K,\mathrm{act}} \Big(\lambda_K \big(\Pi_\lambda^h \delta g_n\big)_K + \delta \lambda_K \big(\Pi_\lambda^h \delta g_n\big)_K \Big) K_K.$$

At the discrete level we proceed as follows:

- We have $\sum_{K,\mathrm{inact}} \delta \lambda_K \big(\Pi_\lambda^h g_n\big)_K \leq 0$ for all $\delta \lambda_K$, i.e. $\big(\Pi_\lambda^h g_n\big)_K \geq 0$ a.e. on the inactive part.
- On the active part, it holds that $\sum_{K,\mathrm{act}} \delta \lambda_K \big(\Pi_\lambda^h g_n\big)_K = 0$ for all $\delta \lambda_K$, i.e. $\big(\Pi_\lambda^h g_n\big)_K = 0$ a.e.
- We also impose $\sum_{K,\mathrm{inact}} \lambda_K \big(\Pi_\lambda^h \delta g_n\big)_K = 0$ for all $\big(\Pi_\lambda^h \delta g_n\big)_K$, i.e. $\lambda_K = 0$ a.e. on the inactive boundary.

For further development it is convenient to define the vector of virtual variations and linearisations for the Lagrange multipliers:

$$\delta\boldsymbol{\lambda} = \begin{bmatrix} \delta\lambda_1 \\ \vdots \\ \delta\lambda_{\mathcal{K}} \end{bmatrix}, \qquad \Delta\boldsymbol{\lambda} = \begin{bmatrix} \Delta\lambda_1 \\ \vdots \\ \Delta\lambda_{\mathcal{K}} \end{bmatrix}, \qquad \boldsymbol{N}_{\lambda,g} = \begin{bmatrix} \left(\Pi_\lambda^h g_n\right)_{1,\mathrm{act}} K_{1,\mathrm{act}} \\ \vdots \\ \left(\Pi_\lambda^h g_n\right)_{\mathcal{K},\mathrm{act}} K_{\mathcal{A},\mathrm{act}} \end{bmatrix}, \qquad \boldsymbol{B}_\lambda = \begin{bmatrix} B_1(\zeta) \\ \vdots \\ B_{\mathcal{K}}(\zeta) \end{bmatrix}.$$

In matrix form it holds that

$$\delta W_c = \delta\boldsymbol{u}^{\mathrm{T}} \int_{\Gamma_C} \Big(\sum_{K,\mathrm{act}} B_K \lambda_K \Big) \boldsymbol{N}\, \mathrm{d}\Gamma + \delta\boldsymbol{\lambda}^{\mathrm{T}} \boldsymbol{N}_{\lambda,g},$$

and the residual for the Newton–Raphson iterative scheme is obtained as:

$$R = \begin{bmatrix} R_u \\ R_\lambda \end{bmatrix} = \begin{bmatrix} \int_{\Gamma_C} \left(\sum_{K,\mathrm{act}} B_K \lambda_K\right) \boldsymbol{N}\, \mathrm{d}\Gamma \\ \boldsymbol{N}_{\lambda,g} \end{bmatrix}.$$

The linearisation yields

$$\Delta\delta W_c = \int_{\Gamma_C} \Delta\lambda \delta g_n \, \mathrm{d}\Gamma + \int_{\Gamma_C} \delta\lambda \Delta g_n \, \mathrm{d}\Gamma.$$

The active-set strategy and the discretised contact contribution can be expressed

$$\begin{aligned} \Delta\delta W_c &= \sum_{K,\mathrm{act}} \sum_{A} \int_{\Gamma_C} \Delta\lambda_K B_K N_A \delta u_A \cdot n \, \mathrm{d}\Gamma + \int_{\Gamma_C} \delta\lambda_K B_K N_A \Delta u_A \cdot n \, \mathrm{d}\Gamma \\ &= \delta\boldsymbol{u}^{\mathrm{T}} \int_{\Gamma_{C,\mathrm{act}}} \boldsymbol{N}\boldsymbol{B}_\lambda^{\mathrm{T}} \, \mathrm{d}\Gamma \, \Delta\boldsymbol{\lambda} + \delta\boldsymbol{\lambda}^{\mathrm{T}} \int_{\Gamma_{C,\mathrm{act}}} \boldsymbol{B}_\lambda \boldsymbol{N}^{\mathrm{T}} \, \mathrm{d}\Gamma \, \Delta\boldsymbol{u}. \end{aligned}$$

REMARK A1 The term $\Delta\delta g_n$ has been removed from the linearisation strategy as it has the undesired effect of deteriorating the convergence of the Newton scheme in almost all cases of interest.